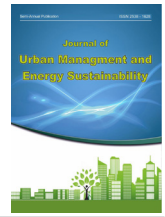
International Journal of Urban Management and Energy Sustainability (IJUMES)

Homepage: http://www.ijumes.com



CASE STUDY RESEARCH PAPER

An intelligent approach using the experimental study of geopolymer self-compacted concrete and implementing an intelligent image processing techniques for the rehabilitation of building

Mansour Keshavarzi[1], Towhid Pourrostam[2*], Mohammad Reza Javaheri Tafti[1]

1 Department of Civil Engineering, Taft. C., Islamic Azad University, Taft, Iran

2 Department of Civil Engineering, CT.C., Islamic Azad University, Tehran, Iran*

ARTICLE INFO

Article History:
Received 2026-01-04
Revised 2026-03-08
Accepted 2026-05-25

Keywords:
Fiber reinforcement; ground granulated blast furnace slag; image processing; Self-compacting geopolymer concrete; shrinkage

ABSTRACT

Self-compacting geopolymer concrete can reduce the carbon footprint of concrete construction while removing the need for vibration, but the effects of fiber reinforcement on its hardened properties and shrinkage, and practical tools for checking the composition of hardened geopolymer concrete, remain limited. This study evaluated GGBS-based SCGPC reinforced with steel fibers, polypropylene fibers and their hybrid combination and compared it with corresponding self-compacting concrete mixtures. Twelve mixtures were tested for water absorption, compressive and splitting tensile strength at 7 and 28 days, and drying shrinkage. In addition, an image-processing procedure based on HSV colour segmentation and pixel counting in Python was developed to quantify the phases exposed on sawn sections of hardened geopolymer concrete. SCGPC showed lower water absorption and lower shrinkage than SCC. With 1% steel fibers, SCGPC reached 36.03 and 40.04 MPa at 7 and 28 days, 4.4% and 1.9% higher than the steel-fiber SCC, and showed the lowest shrinkage. PP fibers slightly reduced the 7-day strength, and the hybrid mixture had a 28-day strength 8.4% lower than its SCC counterpart. The geopolymer mixtures reached splitting tensile strengths of 3.0–3.8 MPa, compared with 2.9–3.3 MPa for SCC. Image analysis separated bright and dark regions, covering 71.15% and 28.85% of the section, respectively. Fiber-reinforced SCGPC, particularly with steel fibers, is therefore a viable low-shrinkage alternative to SCC, and image analysis offers a rapid, low-cost means of checking hardened geopolymer concrete in rehabilitation assessments.

DOI: 10.22034/ijumes.2026.743890

Running Title: Geopolymer self-compacted concrete and implementing an intelligent image processing techniques

NUMBER OF REFERENCES 40

NUMBER OF FIGURES 14

NUMBER OF TABLES 04

*Corresponding Author:
Email: *t.pourrostam@iau.ac.ir*
Phone: 00983532628000
ORCID: https://orcid.org/0000-0002-3981-4111

INTRODUCTION

Self-Compacting Concrete (SCC) has been widely embraced in the construction sector since the 20th century, mostly driven by extensive industrialization and a scarcity of operative workers. SCC is a unique type of high-performance concrete that can adequately fill voids under its own weight without the need for vibration or compaction. The high performance SCC mixtures guarantees the performance criteria both in its fresh and hardened condition (Al-Oran et al., 2022; Aslani & Nejadi, 2012; Khayat & De Schutter, 2014; Persson, 2001). Both high flow ability and stability of the paste must be achieved in its fresh form to prevent the segregation of coarse particles. Furthermore, the structural integrity of SCC must be met in its hardened condition. EFNARC has established criteria and requirements for the components utilized, diagnostic techniques, and other technical elements in self-compacting concrete (SCC). The key attributes of SCC are its capacity to fill, enable passage, and prevent segregation. Attaining this objective requires a methodical selection of the elements (Brouwers & Radix, 2005). The permitted powder content must not exceed 600 kg/m3, whereas the maximum coarse aggregate concentration should not exceed 1000 kg/m3. The fine aggregate component constitutes typically 48-55% of the overall weight of the aggregate. The water content ranges from 150 to 210 kg/m3. In addition, a superplasticizer and viscosity modifying additive are included in the option to meet the requirements of self-compacting concrete (Aggarwal et al., 2008; Domone, 2006). Standard powder binding materials used in SCC include ordinary Portland cement and fly ash (Corinaldesi & Moriconi, 2011; Kavitha & Kala, 2016; Selvarani & Preethi, 2021). Nevertheless, the process of cement manufacturing incurs significant use of natural resources and results in substantial emissions of CO2, therefore giving rise to grave environmental concerns. To decrease the reliance on cement in concrete, experts are exploring several suitable alternatives. Professor Davidovits introduced geopolymer technology in the late 1970s as one of several alternative solutions (Davidovits, 1991). While other options somewhat substitute cement, geopolymer fully removes the need of cement in concrete. By mixing alkali hydroxide and/or alkali silicate activators with reactive alumina silicate solid powder such as fly ash or micro silica, geopolymer is a solid and stable inorganic substance composed of alumina silicate (Davidovits, 1991). An alkali alumina silicate gel, referred to as the geopolymeric gel binder phase, is formed when alumina silica solid material reacts with alkaline activators. Geopolymer concrete presents promising prospects for widespread usage due to its minimal greenhouse gas emissions during manufacturing and its comparable applicability to Portland cement concrete in the building industry (Almutairi et al., 2021; Islam et al., 2015). Considerable research has been conducted utilizing various industrial byproducts and natural alumina silica abundant elements in geopolymer concrete (Mehta & Siddique, 2018; Nagajothi & Elavenil, 2021; Patil et al., 2018; Reddy et al., 2018; Sireesha & Madhavi, 2018; Verma & Dev, 2022). Numerous researchers have endeavored to develop Self-Compacted Geopolymer Concrete (SCGPC) as part of the ongoing investigation of GPC. Previous research has documented the advancement of self-compacting geopolymer concrete utilizing fly ash, GGBS, silica fume, rice husk ash, and other similar materials (Patel & Shah, 2018; Saini & Vattipalli, 2020; Vishnu et al., 2021). Indeed, self-compacting geopolymer concrete is a highly fluid substance. Given the crucial significance of self-compact ability, it is important to carefully choose and determine the appropriate dosage of superplasticizer in SCGPC (Praveen & Srinivasan, 2017). Highly suggested for achieving the appropriate self-compacting properties in SCGPC is a superplasticizer based on poly carboxylic ether (Kalyana Rama et al., 2015; Kumar et al., 2021; Luo et al., 2024; Vishnu et al., 2021). Nevertheless, more water is recommended to enhance the workability of GPC, without sacrificing the necessary strength characteristics. Yet,

an excessive amount of water leads to bleeding and segregation, resulting in a reduction in the impressive compressive strength. Further water addition does not contribute to any reaction in SCGPC (Al-Oran et al., 2022). Additional research has indicated that augmenting the concentration of GGBS with a lower amount of activator leads to decreased flow ability and setting time (Faridmehr et al., 2021; Kalyana Rama et al., 2015; Rahman & Al-Ameri, 2021; Ramineni et al., 2018; Reddy & Elavenil, 2017). As the molarity of NaOH increases, the viscosity and flow ability properties of SCGPC tend to decrease (Arun et al., 2019; Praveen & Srinivasan, 2017; Vinothkumar et al., 2019). Yet, the increased concentration of NaOH reduces the self-compacting properties; the compressive strength was seen to rise in fly ash and GGBS based self-compacting glass powder concrete (Al-Oran et al., 2022). Rapid dissolving of alumina silicate glasses is induced by a larger concentration of NaOH, resulting in increased strength (Nagaraj & Venkatesh Babu, 2018). In the next step of this study, the coupling of the image processing techniques and artificial intelligence methods is implemented for an intelligent approach to estimate the geopolymer concrete mixture proportion. Using concrete with a suitable strength and other utility qualities is one of the prerequisites for the safe usage of concrete constructions. There exist many methodologies for establishing the proportions of concrete mixtures prior to construction. Nevertheless, there is a clear absence of a thorough protocol for ascertaining the proportions of concrete mixtures following the process of mixing and hardening. This procedure is often necessary to assess the concrete mixture proportions for several reasons, including accuracy control in concrete production and general quality assurance, evaluation of the causes of inadequate performance of hardened concrete, and determination of the properties of concrete before damage occurs by access to the damaged concrete. These procedures are often conducted in cases of disagreement when there is suspicion of non-compliance with the blending proportions. To address the absence of a dedicated strategy, this study devised an image analysis-based approach to recover concrete mixture proportions from hardened concrete. Digital image processing has emerged as a valuable tool in several civil engineering domains, including the evaluation of moisture susceptibility in asphalt mixtures, the assessment of concrete surface quality, the consideration of concrete pore structure, and the analysis of the microstructure of the interfacial transition zone (ITZ). These examples provide a limited selection of potential uses. For the analysis of aggregate properties in 2D photographs of cured concrete, it is necessary to initially isolate aggregates from cement paste. The grey hue of paste embedded in cement concrete diminishes the distinction between it and aggregates, resulting in reduced precision in the separation of aggregates

Based on the literature reviewed, several research has been conducted to determine the mixing proportions from hardened concrete of unknown composition. Nevertheless, each research only assessed certain combination proportions, thereby lacking a comprehensive analysis that encompasses all blending proportions of traditional concrete. Particularly when the calculation of a parameter related to the proportions of a mixture relies on another parameter related to the proportions of the mixture (for example, the quantification of binder content is influenced by the ratio of solution to binder), it is crucial to assess the overall reliability of the approach. The present study originally introduces a novel and all-encompassing approach for obtaining combination proportions from hardened geopolymer concrete (GPC). Images depicting the macrostructure of GPC were employed for this analysis. Firstly, the volume ratios of aggregates, binder paste, and air spaces may be calculated by establishing suggested correlations between the mass and volume of concrete phases and the components of hardened cement. Moreover, the binder content was determined using a suggested equation derived from the equilibrium state of

alkaline solution, binder, and binder paste. This simulation was based on the estimated volume ratio of binder paste and the estimated solution to binder ratio. Therefore, by employing the proposed techniques in this attempt, it is possible to estimate the volume ratios of aggregates, binder paste, and air voids, as well as the aggregate size distribution, solution to binder ratio, binder content, and alkaline solution content for an unidentified hardened GPC. (Fig. 1) illustrated of the step-by-step of the image processing and modeling of the GPC mixtures.

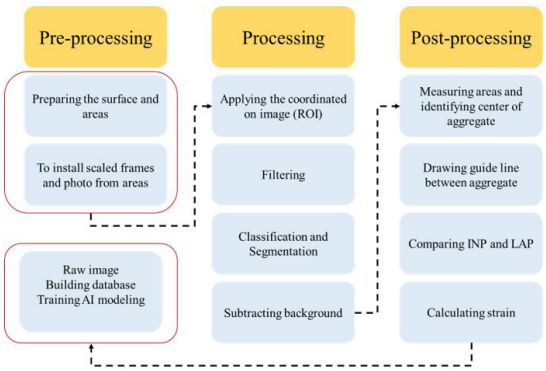


Figure1: Preparation of image processing analysis

MATERIALS AND METHIODS

Experimental program

In this section, the materials and mix design preparation is presented.

Material specifications

(a)The GGBS with a granule density of 2.66 g/cm3 was sourced from Foolad Mobarakeh in Esfahan. The combined concentration of Al2O3, SiO2, and Fe2O3 in the GGBS was 50.81% (Tab. 1). The ASTM C618 threshold of 70% applies to fly ash and natural pozzolans; GGBS is specified by ASTM C989 and is characterised mainly by its high CaO content (34.07%). Table 1 provides the chemical characteristics and loss on ignition (LOI) of the specific pozzolans that were employed. In the provided table, the rounding of the data results in a sum of the percentages of various components that does not equal 100%. Finally, Fig. 2 shows the X-ray diffraction (XRD) pattern of the GGBS used (Stutzman, 2003).

Table 1: Chemical composition of utilized materials (%)

Component (%)	C	LSP	GGBS
SiO2	21.9	0.45	32.57
Al2O3	4.86	4.86	16.98
Fe2O3	3.30	3.30	1.26
CaO	63.33	63.33	34.07
MgO	1.15	1.15	9.69
SO3	2.10	2.10	0.84
Loss of ignition (LOI)	2.40	-	0.39

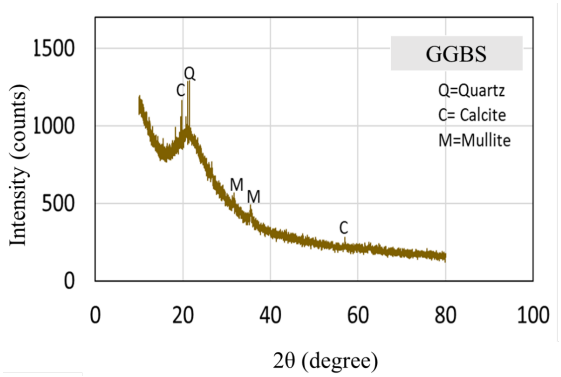


Figure 2: XRD test for utilized GGBS

(b)Alkaline solution

The activating agent for the solid precursor was an alkaline solution consisting of glass water (sodium silicate or Na2SiO3) and sodium hydroxide (NaOH). Sodium hydroxide flakes of 96% purity were dissolved in water to prepare the NaOH solution. The SiO2 / Na2O ratio of the sodium silicate solution used in this study was 2.27 (SiO2 = 35.9%, Na2O = 15.8%).

(b)Fibers

An experimental study was conducted to produce environmentally friendly structural geopolymer concrete (GPC) mixtures utilizing a combination of steel (ST) and polypropylene (PP) fibers manufactured at Sepahan Aliaf Company in Esfahan, Iran. Table 2 provided the specific parameters of the fibers employed. The

geopolymer composite was reinforced using a 6 mm length PP fiber. In this investigation, the best mixes were developed using hooked-end steel fibers with a maximum length of 5mm and a diameter of 0.12 mm. To achieve this, PP at concentrations of 0.75, 1, 1.25 vol%, and St at 2 vol% were included into the GPC mixture combinations.(Tab. 2)

Table 2: Fiber properties

	PP	ST
Length (mm)	6	12
Density (gr/cm3)	0.93	7.8
Tensile strength (MPa)	400	2500
Water absorbency	No	No
Alkaline and acid resistance	Excellent	Excellent
Diameter (mm)	-	0.12

(c)Aggregates

The concrete volume was comprised of approximately 67% fine aggregates (FA) and 33% coarse aggregates (CA) by mass of total aggregate. The fine aggregate comprised of natural sand obtained from a nearby quarry with a fineness modulus of 3.05, falling within the acceptable range specified by ASTM C33 (Berney & Smith, 2008). The upper limit of grain size for the used CA was 12.5 mm. Moreover, the specific gravity and water absorption values were recorded as 2.57 and 1.52% correspondingly. In Table 3, the sieve analyses for the coarse and fine aggregates are presented.(Tab. 3)

Methodology

Mix design, sample preparation and testing process

Figure 3 illustrates the preparation of SCGPC mixes in a mixer. To achieve this objective, the dry ingredients, including CA, FA, and SCMs, were mixed in the mixer for up to 3 minutes. Then, the alkaline solution was added and the wet mixing was continued for 4 to 6 minutes until a homogeneous mixture was achieved. The fresh mixtures were poured into steel cube molds measuring 150×150×150 mm and cylindrical specimens measuring 100×200 mm. The molds were filled in two layers and each layer was subjected to vibration for about 25 seconds onto a vibrating table. The mixture design of reinforced SCGPC mixes is presented in (Tab. 4 and Fig. 3).

Table 3: CA and FA sieve analyses for SCGPC

CA	Sieve size (mm)	12.5	8	5.75	4	2	1
	Passing percentage (%)	100	76	47	22	4	2
FA	Sieve size (mm)	9.5	4.75	2.36	1.18	0.6	0.3
	Passing percentage (%)	100	87.6	63.5	41.9	23.3	4.5



Figure 3: The SCGPC specimens

Figure 3 shows that the prepared specimens were placed in an oven set at a temperature of 60 0C for a duration of 24 hours. The specimens were then taken out of the molds and cured at a temperature of 24 ± 2 ◦C and a relative humidity of 20% ± 2% until they reached the required temperature as per the ISO-834 standard fire curve for testing purposes. After curing for 28 days, four cubical specimens and two cylindrical tests were conducted to evaluate the strength of STS and MoE, following the specifications of

BS EN 12390-3 and ASTM-C496-11, respectively (Rodriguez et al., 1994). The Module of elasticity (ME) was assessed on the 28th day using the cylindrical test technique as specified in ASTM-C469–14. For assessing the post-fire performance of the SCGPC. A controlled temperature furnace was used to expose the specimens to elevated temperatures. The furnace underwent heating at a rate of 10 ◦C per minute, and the temperature reached remained constant for a duration of two hours. Next, the furnace was deliberately cooled at a rate of 1.62 ◦C/min to avoid any thermal shocks that may potentially impact the specimens. All the mixes shown in Table 4 featured a constant water-to-solids ratio of 0.48. The water composition included both the mixing water and the water containing NaOH and Na2SiO3. Furthermore, the solid materials consisted of GGBS, Fly ash and MS, as well as the solid component of the NaOH and Na2SiO3 solutions. Furthermore, the concentration of the sodium hydroxide solution was 6 Molar, and the Na_2SiO_3/NaOH ratio was 2.5. The effect of employed SCMs and fibers on the SCGPC properties was studied by producing 12 mixes. In these mixtures, Fly ash and MS were substituted by 0%, and 11% SCMs by weight.

Table 4: Mixture proportions of reinforced SCGPC

Sample ID	W	SCMs	C	GGBS	CA	FA	Fiber (%Vf)	Solution to binder ratio
OPC	200	295	295	-	500	1036	0	-
SCC	200	295	295	-	500	1036	0	-
SCCST	200	295	295	-	500	1036	1% ST	-
SCCPP	200	295	295	-	500	1036	1%PP	-
SCCSTPP	200	295	295	-	500	1036	0.5%ST+0.5PP	-
GSCGPC	121	295	-	295	500	1036	0	0.4
FSCGPC	121	295	-	295	500	1036	0	0.4
MSCGPC	121	295	-	295	500	1036	0	0.4
SCGPC	121	295	-	295	500	1036	0	0.4
SCGPC ST	121	295	-	295	500	1036	1%ST	0.4
SCGPC PP	121	295	-	295	500	1036	1%PP	0.4
SCGPCSTPP	121	295	-	295	500	1036	0.5%ST+0.5PP	0.4

FINDINGS AND DISCUSSION

Water absorption

Ordinary Portland cement concrete (OPC) is a water-based composite. Aggregates, which are the main structure of concrete, are connected to each other with the help of cement and form a dense and relatively integrated structure. Cement plays the role of adhesive in this process. Cement particles are hydrated during the reaction with water and turn into a strong adhesive during chemical reactions. This chemical process is called hydration. C-S-H calcium silicate hydrate is the result of cement hydration process. For the chemical reactivity of cement, water is needed in the amount of 25% of its weight. This amount of water is not enough to lubricate the concrete and we have to use more than this amount of water. According to the studies, whatever water is consumed more than 25 percent by weight of cement, it will gradually evaporate from the structure and form micro and capillary holes. These holes are the main absorption factor in the concrete structure. Depending on the type of application of concrete, its water absorption should be controlled. Unlike ordinary Portland concrete, the study identified that less water absorption in GPC, which is pre-

sented in (Fig. 4). The GPC-based concrete has the minimum amount of water absorption and the minimum rate of capillary absorption of water compared to OPC (Safiuddin et al., 2011).

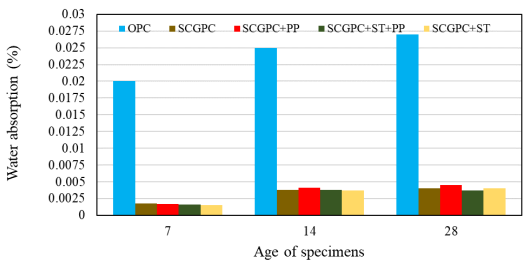


Figure 4: Water absorption of the SCC and SCGPC samples.

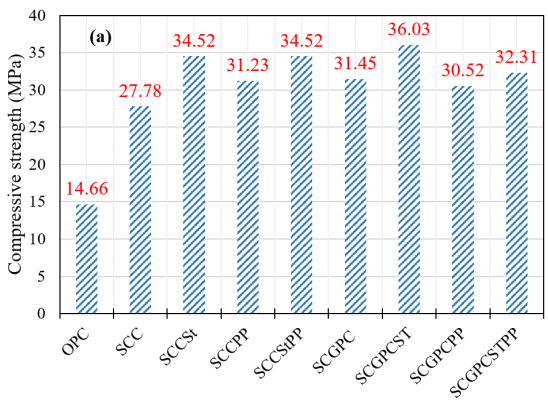
Compressive strength

For each SCC and SCGPC composite, 12 cube specimens were examined in accordance with the ASTM C39 standard (ASTM International, 2017), with three specimens picked for the 28-day experiment. Based on the experimental data presented in (Fig. 5), the compressive strength (CS) of the GPC varies, as do the contents and quantities of the SCMs and fiber content.



Figure 5: CS test procedure of the SCC, GPC and SCGPC specimens

Figure 6 presented the CS results of SCC and SCGPC mixtures in terms of different lengths of PP fibers at the age of 7 days. In general, increasing or decreasing the percentage of fibers in the preparation of concrete will not have much effect on the CS of concrete, but changes in the length of fibers can definitely affect the mechanical performance of concrete samples. In this study, the increase of 0.5% PP fibers and 0.5% steel has caused changes in the CS of concrete. For example, the use of PP fibers with a length of 6 mm has the most optimal size in terms of strength in the construction of GPC in comparison to the GSCC+ST mixture. It reached 36.03 MPa at 7 days and 40.04 MPa at 28 days. In SCGPC specimens, adding 10-15% more fibers than SCC mixtures has the conditions to improve compressive strength performance. Based on Fig. 6, the trend of geopolymerization in SCC mixtures for steel blends has increased, but the CS has decreased in mixtures without fibers and containing PP. The CS of GPC is up to 90% in the first three days. The type of activator base material and the processing method in GPC are very important in the CS variation. In the comparison made between two GPC and OPC, it was found that the strength of GPC is higher than OPC at early ages and that is because of the structure of geopolymer concrete. According to Fig. 5, the results of the CS evaluation presented that in 7 days and 28 days, the CS of the fiber reinforced GPC samples improved by 4.4% and 1.9% compared to the steel-fiber SCC. In this study, the sample contains 1% steel fibers manifested the aforementioned strength situation. Contrary to this issue, in samples containing PP fiber, this trend has been decreasing. (Fig, 6)



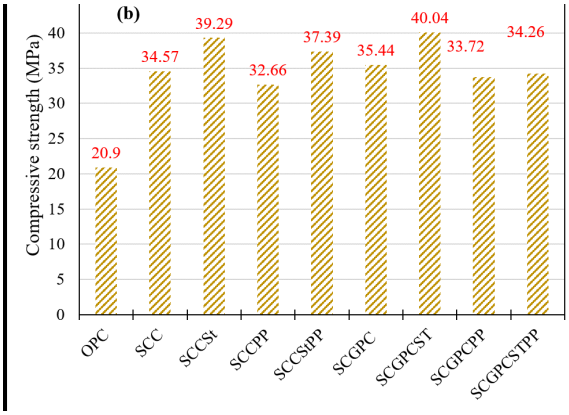


Figure 6: Compressive strength result of SCC, GPC and SCGPC mixtures; (a): 7days, (b): 28days

Tensile strength

The experimental results of the tensile strength for SCC, GPC and SCGPC mixtures with NaOH/Sodium ratios of 2.5 was illustrated in (Fig. 7). The obtained results presented that according to the obtained tensile strength and the overlap of the results, ternary SCGPC mixtures containing PP and hooked-end steel fibers (called SCGPC+ST+PP) have the highest strength. The tensile strength is 249.31 kg/m2 with all different ratios of NaOH/Sodium. For example, for the ratio of sodium hydroxide to sodium equal to 2.5, the samples made with geopolymeric fibers have reported better mechanical conditions due to polymer binding and better engagement. The amount of adhesion of geopolymer concrete is higher than that of ordinary concrete, and this adhesion is directly related to their compressive strength. In fact, the factors in GPC that affect its strength also increase its adhesion. The convergence rate of compressive and tensile strength results in this study was 87%. The results indicated that GPC had excellent tensile strength to withstand bending in structural elements. The SCGPC mixtures with steel fibers is an economical option for solving the structural issues in fractured portions of concrete elements. The use of steel fiber reinforcement in concrete enhances the capacity of structural elements to bear substantial loads. In accordance with the guidelines of ACI Committee 544, geopolymer concrete reinforced with steel fibers is employed as an addition to mitigate stress cracking, enhance resistance to impact or dynamic loading, and reduce material waste. Furthermore, the study found that combinations including steel fibers in self-compacting geopolymer (SCGPC+ST+PP) and self-compacting concrete including steel fibers (SCC+ST) exhibited greater 28-day tensile strength

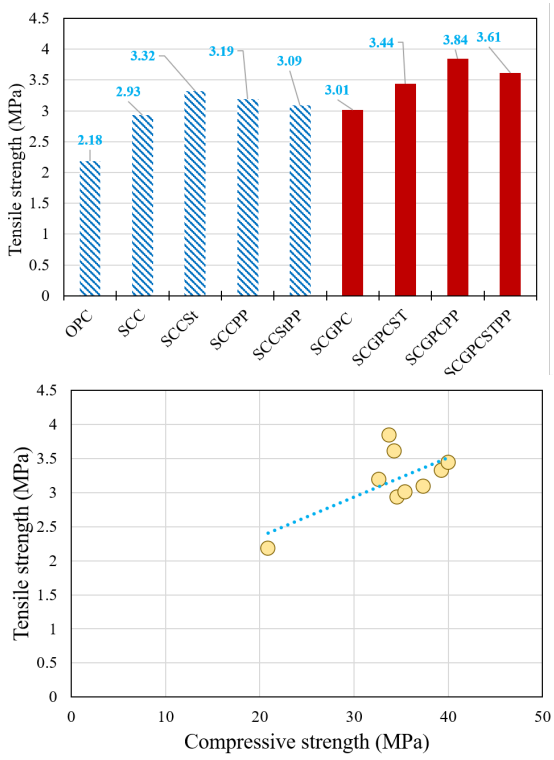


Figure 7: Tensile strength result of SCC, GPC and SCGPC mixtures;

Shrinkage

The concrete shrinkage test in this study was conducted following the procedure. This phenomenon is referred to as concrete shrinkage. Constant variation in volume is a highly detrimental characteristic of concrete. Engineering speaking, the modification of concrete volume is significant as it leads to the formation of unsuitable fissures in the concrete. These fractures

impact its structural integrity and extended lasting resilience. Concrete shrinkage refers to the gradual reduction in the volume of concrete during time, resulting in a decrease in its dimensions. In hardened concrete, shrinkage is the consequence of moisture loss. Vacancy of tiny holes in concrete leads to the generation of negative capillary pressure, therefore decreasing the volume of the concrete. This phenomenon is the process of water evaporation from the surface of recently mixed concrete or its absorption into the concrete or substrate. Hydraulic contraction is a reduction in volume caused by the migration of water from the concrete during its plastic or pre-set condition. Water migration can occur either during the hydration process or due to environmental factors causing water to evaporate on the wet concrete surface. Thus, the higher the bleeding of the concrete, the more significant the plastic shrinkage should be. The extent of this shrinkage is contingent upon the quality of the cement. Studies on the w/c ratio indicate that the weight ratio of water to cement in the concrete mixture is inversely proportional. (Fig. 8) shows the shrinkage results obtained in this work. The present work involved the fabrication of 9 samples to examine the pattern of moisture decrease in self-compacting and self-compacting geopolymer samples during a 25-day timeframe. This test is conducted under controlled settings, including regulated temperature and humidity, on predetermined samples. The implementation of geopolymer has resulted in a reduction in the level of shrinkage in the blended materials. The concrete shrinkage test was conducted using a device designed to measure the shrinkage of self-compacting geopolymer concrete, as shown in (Fig. 9), following the ISI8592 standard protocol.

The utilization of fibers in the production of self-compacting and self-compacting geopolymer substrates has declined. Steel fibers exhibit a mechanism for managing cracking in both drying shrinkage and plastic shrinkage during restricted shrinkage tests. In conjunction with

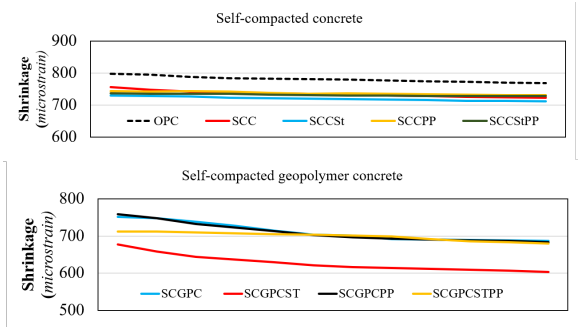


Figure 8: Shrinkage of SCC and SCGPC mixtures

non-shrinkage cements, steel fibers can serve as an effective mechanism for restricting cracks, therefore enabling concrete to achieve its crack control function even in the absence of traditional reinforcing (Sargaphuti et al., 1993). Synergistic approaches involving steel fibers and non-shrinking cements have been employed. One factor contributing to the formation of fractures resulting from plastic shrinkage is the reaction of concrete water with particles. The deposition of aggregates or reinforcements results in the formation of fractures either on the surface of the structure or within the aggregate compartments. The data presented in Fig. 9 clearly demonstrates a reduction in the moisture content in all test samples of concrete. In this study, the lowest shrinkage was achieved by SCGPC+ST mixture (from 677 micro strain to 603 micro strain). The phenomenon of drying shrinkage arises from the depletion of surface adsorbed water from the calcium silicate hydrate (C-S-H) gel and the reduction of hydrostatic tension within the tiny pores. Swelling is the opposite of shrinkage. The primary cause of this shrinkage is the distortion of the concrete paste. The hardness of the aggregate significantly influences it. The majority of drying shrinkage instances manifest within the initial months of the concrete structure's lifespan. The extraction of water from the concrete, which is retained in the unsaturated air spaces, results in dry shrinkage.

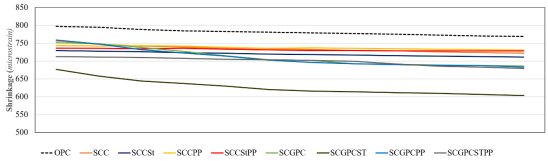


Figure 9: Comparison between the shrinkage of SCC and SCGPC mixtures

Image processing evaluation

The image processing procedure employed to estimate the aggregate content in concrete specimens involves several key stages that must be carried out with precision. The following presents a step-by-step explanation of the workflow:

Preparation and Preprocessing

Step 1: Specimen Preparation

•As illustrated in (Fig.10), before conducting image processing, it is essential to properly prepare the concrete specimens.

•Sample Cutting: If the specimens are cylindrical or cubic, an appropriate cross-sectional surface must be prepared for imaging.

•Surface Polishing: To improve the accuracy of the analysis, the concrete surface should be smooth and uniform to obtain a clearer image of the aggregates.

•Surface Cleaning: The specimen surface must be free of dust and debris to prevent image distortion and preserve details.



Figure 10: Sample preparation before implementing image analysis (Source: Keshavarzi et al., 2026)

Step 2: Image Acquisition

•At this stage, suitable images of the cross-sectional surfaces of the specimens are captured.

Camera Selection: High-resolution cameras equipped with proper sensors are used for capturing the specimen surfaces.

•Lighting Adjustment: Lighting should be uniform and shadow-free. Indirect lighting and optical filters can enhance contrast.

•Image Format: Images are saved in lossless formats such as TIFF or PNG to minimize quality degradation.

Step 3: Image Preprocessing

As shown in (Fig. 11), the geopolymer specimen was initially photographed, and preliminary preprocessing was carried out to enhance image quality and reduce noise. The following steps were implemented accordingly [reference missing]:

•Grayscale Conversion: If the image is colored, it is converted to grayscale.

•Contrast Enhancement: Methods such as histogram equalization are applied to improve the distinction between aggregates and the cementitious matrix.

•Noise Reduction: Smoothing filters are used to reduce noise.

•Edge Enhancement: Filters such as the Canny Edge Detection method are employed to detect aggregate boundaries.

Subsequently, aggregates are separated from the cementitious matrix using the following methods:

Thresholding: Defining a threshold value to distinguish image regions.

•Image Segmentation: Implementing Watershed Segmentation techniques.

•Boundary Refinement: Reviewing and correcting separated boundaries.

•Connected Component Labeling: Identifying the number and location of aggregates.

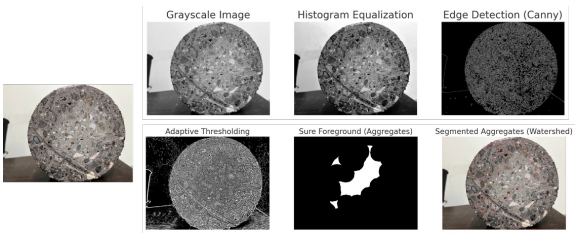


Figure 11: Image analysis preprocessing steps (Source: Keshavarzi et al., 2026)

Aggregate Feature Extraction

Evaluating the proportions of aggregates and cement substitutes (slag, in this study) in concrete specimens through image processing typically includes several essential steps. The cross-sectional images of the concrete are used to identify and separate material phases (aggregate, binder, and voids). The following procedures were conducted:

•Connected component analysis to count the number of aggregates.

•Determination of the area of each aggregate by assessing connected pixels.

•Calculation of average aggregate size based on particle size distribution.

Image Analysis Stages

a) Conversion to HSV Color Space

The image is converted from the BGR (Blue-Green-Red) color space to the HSV color space. This conversion improves color recognition accuracy and simplifies processing.

b) Defining Color Ranges

Color ranges in the HSV space are defined for each component (gravel, sand, and slag) according to their observed color values in the image. In this study, the color range parameters were as follows, and Figure (12) illustrates their determination on concrete surfaces:

• Gravel: Hue range between 20 and 30.

•Sand: Hue range between 10 and 20.

•Slag: Value range between 100 and 255 (to detect brighter areas).

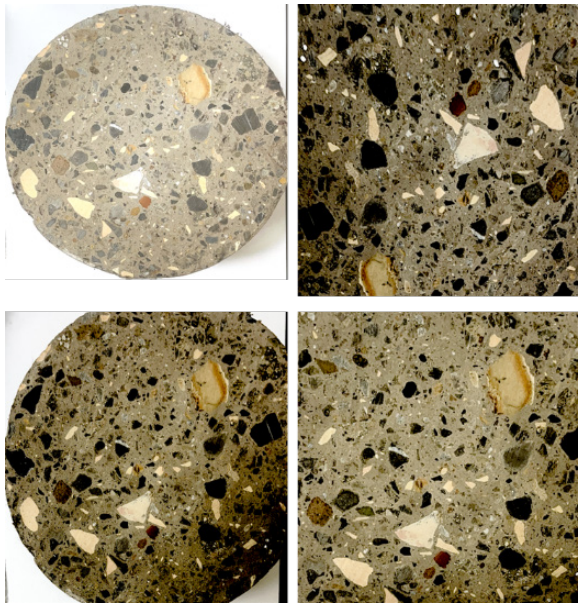


Figure 12: Determining the color range in the surface of geopolymer concrete slabs (Source: Keshavarzi et al., 2026)

c) Mask Generation

For each component, a binary mask is created where the corresponding pixels are assigned white (255) and all others black (0). These masks were generated in Python using the cv2.inRange function.

d) Pixel Counting

The number of white pixels in each mask represents the area occupied by that component. (Fig. 13) demonstrates the black-and-white pixel processing used in this evaluation. Three major image representations were analyzed:

Original Image: The raw cross-sectional image of the geopolymer concrete specimen, showing all components aggregates (gravel and sand), slag, and the cementitious matrix. Color variations correspond to differences in chemical composition and texture.

Processed Image: After applying techniques such as grayscale conversion or contrast enhancement, components are visually distin-

guished based on optical characteristics, allowing more accurate analysis.

Binary Image: The final processed image divides components into two major regions bright areas (aggregates and slag) and dark areas (matrix). This binary format facilitates quantitative analysis, such as measuring aggregate area percentages and their spatial distribution.

e) Coverage Percentage Calculation: The coverage percentage of each component is computed using the following formula:

$$\text{Percentage coverage} = \frac{\textit{Number of pixels}}{\textit{Total number of pixels in the image}} \quad (1)$$

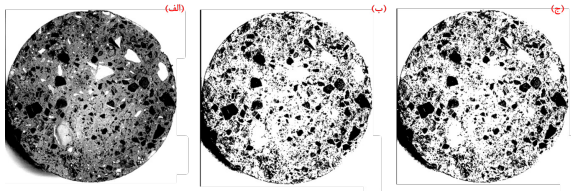


Figure 13: Creating white and black pixels in geopolymer concrete sample processing (Source: Keshavarzi et al., 2026)

Image Analysis Results

Based on image processing, the percentage areas of gravel, sand, and slag were determined by image segmentation and pixel counting. The corresponding pseudo-code used for this analysis is illustrated in (Fig. 14).

According to the image processing results, the coverage percentages of different components in the geopolymer concrete specimen were as follows:

•Bright Regions (aggregates and slag): 71.15% of the total surface area.

•Dark Regions (cementitious matrix): 28.85% of the total surface area, representing the alkaline binder and water phase.

These percentages reflect the relative distribution of materials within the concrete specimen. The bright regions typically include aggregates (gravel and sand) and slag embedded in the matrix. Further analysis of the bright regions yielded the following detailed results:

• Gravel: 34.25%

This indicates that gravel occupies 34.25%

```python
import cv2
import numpy as np

def analyze_concrete_image(image_path):
    # بارگذاری تصویر
    image = cv2.imread(image_path)
    hsv = cv2.cvtColor(image, cv2.COLOR_BGR2HSV)

    # تعیین محدوده‌های رنگی برای شن، ماسه و سیمان
    lower_sand = np.array([20, 100, 100])  # محدوده رنگ شن
    upper_sand = np.array([30, 255, 255])

    lower_gravel = np.array([10, 50, 50])  # محدوده رنگ ماسه
    upper_gravel = np.array([20, 255, 255])

    lower_cement = np.array([0, 0, 100])   # محدوده رنگ سیمان
    upper_cement = np.array([180, 50, 255])

    # ایجاد ماسک‌ها برای هر جزء
    mask_sand = cv2.inRange(hsv, lower_sand, upper_sand)
    mask_gravel = cv2.inRange(hsv, lower_gravel, upper_gravel)
    mask_cement = cv2.inRange(hsv, lower_cement, upper_cement)

    # شمارش پیکسل‌های هر جزء
    sand_pixels = cv2.countNonZero(mask_sand)
    gravel_pixels = cv2.countNonZero(mask_gravel)
    cement_pixels = cv2.countNonZero(mask_cement)

    # محاسبه درصد پوشش
    total_pixels = image.shape[0] * image.shape[1]
    sand_percentage = (sand_pixels / total_pixels) * 100
    gravel_percentage = (gravel_pixels / total_pixels) * 100
    cement_percentage = (cement_pixels / total_pixels) * 100

    return sand_percentage, gravel_percentage, cement_percentage

# تحلیل تصویر
image_path = 'concrete_sample.png'  # مسیر تصویر بتنی
sand_percent, gravel_percent, cement_percent = analyze_concrete_image(image_path)
print(f"Sand = {sand_percent:.2f}%, Gravel = {gravel_percent:.2f}%, Cement = {cement_percent:.2
f}%")
```

Figure 14: Python pseudocode used in this study

of the image surface, representing an adequate aggregate proportion contributing to concrete strength and durability.

• Sand: 35.67%

Sand covers 35.67% of the surface area, acting as a filler that enhances concrete compaction and uniformity.

• Granulated Blast Furnace Slag: 30.67%

This value shows that slag (used as a binder replacement) accounts for 30.67% of the surface area. The appropriate slag ratio contributes to the cohesive and binding properties of the concrete matrix.

RESULTS AND CONCLUSION

The mechanical and shrinkage behavior of a fiber reinforced self-compacted geopolymer concrete (SCGPC) containing GGBS, fly ash, and MS was investigated in this study. A series of mixes were prepared and evaluated by investigating workability performance and fiber consumption of geopolymer concrete. The following result were obtained for this study:

•The results of compressive strength (CS) evaluation presented that in 7 days and 28 days,

the CS of reinforced SCGPC mixture improved by 4.4% and 1.9% compared to the steel-fiber self-compacted concrete, which is clearly evident in samples containing 1% of steel fibers.

•The results of evaluating the resistance properties in the mixtures containing polypropylene also indicated that in 7 days and 28 days, the CS of the SCGPC samples was reduced by 2.3% at 7 days and increased by 3.2% at 28 days compared to the PP-fiber self-compacted concrete (1% PP fibers).

•The results of samples containing both steel and polypropylene fibers also showed that the 28-day CS of reinforced SCGPC was 8.4% lower than that of the corresponding hybrid-fiber self-compacted concrete.

•The splitting tensile strength of the SCGPC mixtures (3.01–3.84 MPa at 28 days) exceeded that of the SCC mixtures (2.93–3.32 MPa); the highest value was obtained for SCGPC with PP fibers (3.84 MPa), followed by the hybrid SCGPC (3.61 MPa).

•The results of this study showed that shrinkage in self-compacting slag geopolymer concrete has presented reduced values compared to self-compacting concrete. The steel fibers-based mixtures have shown less shrinkage due to moisture reduction in self-compacting geopolymer concrete compared to polypropylene samples.

•Based on the results obtained, the percentage of aggregates (sand and gravel) and iron furnace slag coverage in concrete samples was 34.25%, 35.67% and 30.67%, respectively. These values indicate a proper distribution of materials in geopolymer concrete, which can help improve the strength and durability of concrete. Also, the use of digital image processing methods and artificial intelligence not only increases the accuracy of the analyses, but also significantly reduces the time and costs associated with manual methods. This study is an important step towards developing accurate and efficient methods for analyzing geopolymer concretes and can play an effective role in expanding the use of these materials in the construction industry. Given the importance of reducing the consumption of natural resources and reducing environmental pollutants, the use of geopolymer concretes and advanced analytical methods can help achieve sustainable development goals in the construction industry.

REFERENCES

Aggarwal, P., Siddique, R., Aggarwal, Y., & Gupta, S. M. (2008). Self-compacting concrete Procedure for mix design. Leonardo Electronic Journal of Practices and Technologies, 12, 15–24.

Almutairi, A. L., Tayeh, B. A., Adesina, A., Isleem, H. F., & Zeyad, A. M. (2021). Potential applications of geopolymer concrete in construction: A review. Case Studies in Construction Materials, 15, e00733. https://doi.org/10.1016/j.cscm.2021.e00733

Al-Oran, A. A. A., Safiee, N. A., & Nasir, N. A. M. (2022). Fresh and hardened properties of self-compacting concrete using metakaolin and GGBS as cement replacement. European Journal of Environmental and Civil Engineering, 26(1), 379–392. https://doi.org/10.1080/19648189.2019.1663268

Arun, B. R., Nagaraja, P. S., & Srishaila, J. M. (2019). An effect of NaOH molarity on fly ash metakaolin-based self-compacting geopolymer concrete. In Sustainable construction and building materials: Select proceedings of ICSCBM 2018 (pp. 233–244). Springer.

Aslani, F., & Nejadi, S. (2012). Mechanical properties of conventional and self-compacting concrete: An analytical study. Construction and Building Materials, 36, 330–347.

ASTM International. (2017). Standard test method for compressive strength of cylindrical concrete specimens (ASTM C39/C39M-17). ASTM International.

Berney, E. S., & Smith, D. M. (2008). Mechanical and physical properties of ASTM C33 sand. U.S. Army Engineer Research and Development Center.

Brouwers, H. J. H., & Radix, H. J. (2005). Self-compacting concrete: Theoretical and experimental study. Cement and Concrete Research, 35(11), 2116–2136. https://doi.org/10.1016/j.cemconres.2005.06.002

Corinaldesi, V., & Moriconi, G. (2011). The role

of industrial by-products in self-compacting concrete. Construction and Building Materials, 25(8), 3181–3186. https://doi.org/10.1016/j.conbuildmat.2011.03.001

Davidovits, J. (1991). Geopolymers: Inorganic polymeric new materials. Journal of Thermal Analysis, 37(8), 1633–1656. https://doi.org/10.1007/BF01912193

Domone, P. L. (2006). Self-compacting concrete: An analysis of 11 years of case studies. Cement and Concrete Composites, 28(2), 197–208. https://doi.org/10.1016/j.cemconcomp.2005.10.003

Faridmehr, I., Nehdi, M. L., Huseien, G. F., Baghban, M. H., Sam, A. R. M., & Algaifi, H. A. (2021). Experimental and informational modeling study of sustainable self-compacting geopolymer concrete. Sustainability, 13(13), 7444. https://doi.org/10.3390/su13137444

Islam, A., Alengaram, U. J., Jumaat, M. Z., Bashar, I. I., & Kabir, S. M. A. (2015). Engineering properties and carbon footprint of ground granulated blast-furnace slag–palm oil fuel ash-based structural geopolymer concrete. Construction and Building Materials, 101, 503–521. https://doi.org/10.1016/j.conbuildmat.2015.10.026

Kalyana Rama, J. S., Reshmi, N., Sivakumar, M. V. N., & Vasan, A. (2015). Experimental investigation and numerical validation on the effect of NaOH concentration on GGBS based self-compacting geopolymer concrete. In V. Matsagar (Ed.), Advances in structural engineering (pp. 1673–1686). Springer India. https://doi.org/10.1007/978-81-322-2187-6_127

Kavitha, S., & Kala, T. F. (2016). Evaluation of strength behavior of self-compacting concrete using alccofine and GGBS as partial replacement of cement. Indian Journal of Science and Technology, 9(22), 1–5.

Keshavarzi, M., Pourrostam, T. & Javaheri Tafti, M. R. (2026). An Integrated Approach for Analyzing and Evaluating Mix Design Proportions and Compressive Strength of Geopolymer Concrete Sections Lacking Technical Data by Integrating Digital Image Processing and Machine Learning. International Journal of Urban Management and Energy Sustainability, 7(3), 362–377. https://doi.org/10.22034/ijumes.2026.743389

Khayat, K. H., & De Schutter, G. (Eds.). (2014). Mechanical properties of self-compacting concrete (RILEM State-of-the-Art Reports, Vol. 14). Springer.

Kumar, B. N., Kumar, G. V., & Rajesh, V. (2021). Development of fly ash–GGBS based self compacting geo-polymer concrete with and without steel fibres. Computational Engineering and Physical Modeling, 4(3), 1–18.

Luo, Y., Yang, L., Wang, D., Zhang, Q., Wang, Z., Xing, M., Xue, G., Zhang, J., & Liu, Z. (2024). Effect of GGBFS on the mechanical properties of metakaolin-based self-compacting geopolymer concrete. Journal of Building Engineering, 96, 110501. https://doi.org/10.1016/j.jobe.2024.110501

Mehta, A., & Siddique, R. (2018). Sustainable geopolymer concrete using ground granulated blast furnace slag and rice husk ash: Strength and permeability properties. Journal of Cleaner Production, 205, 49–57.

Nagajothi, S., & Elavenil, S. (2021). Effect of GGBS addition on reactivity and microstructure properties of ambient cured fly ash based geopolymer concrete. Silicon, 13(2), 507–516. https://doi.org/10.1007/s12633-020-00470-w

Nagaraj, V. K., & Venkatesh Babu, D. L. (2018). Formulation and performance evaluation of alkali-activated self-compacting concrete. Asian Journal of Civil Engineering, 19(8), 1021–1036. https://doi.org/10.1007/s42107-018-0081-9

Patel, Y. J., & Shah, N. (2018). Enhancement of the properties of ground granulated blast furnace slag based self compacting geopolymer concrete by incorporating rice husk ash. Construction and Building Materials, 171, 654–662. https://doi.org/10.1016/j.conbuildmat.2018.03.166

Patil, S., Karikatti, V., & Chitawadagi, M. (2018). Granulated blast-furnace slag (GGBS) based geopolymer concrete—Review. International Journal of Advanced Science and Engineering, 5(1), 879–885.

Persson, B. (2001). A comparison between mechanical properties of self-compacting concrete and the corresponding properties of normal concrete. Cement and Concrete Research, 31(2), 193–198.

Praveen, P. U., & Srinivasan, K. (2017). Self-compacting geopolymer concrete—A review. IOP Conference Series: Materials Science and Engineering, 263(3), 032024. https://doi.

org/10.1088/1757-899X/263/3/032024

Rahman, S. K., & Al-Ameri, R. (2021). A newly developed self-compacting geopolymer concrete under ambient condition. Construction and Building Materials, 267, 121822. https://doi.org/10.1016/j.conbuildmat.2020.121822

Ramineni, K., Boppana, N. K., & Ramineni, M. (2018). Performance studies on self-compacting geopolymer concrete at ambient curing condition. In International Congress on Polymers in Concrete (ICPIC 2018) (pp. 501–508). Springer. https://doi.org/10.1007/978-3-319-78175-4_64

Reddy, C. J., & Elavenil, S. (2017). Geopolymer concrete with self-compacting: A review. International Journal of Civil Engineering and Technology, 8(2), 163–172.

Reddy, M. S., Dinakar, P., & Rao, B. H. (2018). Mix design development of fly ash and ground granulated blast furnace slag based geopolymer concrete. Journal of Building Engineering, 20, 712–722. https://doi.org/10.1016/j.jobe.2018.09.010

Rodriguez, J., Navarro, C., & Sanchez-Galvez, V. (1994). Splitting tests: An alternative to determine the dynamic tensile strength of ceramic materials. Journal de Physique IV, 4(C8), 101–106.

Safiuddin, M., Mahmud, H. B., & Jumaat, M. Z. (2011). Efficacy of ASTM saturation techniques for measuring the water absorption of concrete. Arabian Journal for Science and Engineering, 36(5), 761–768.

Saini, G., & Vattipalli, U. (2020). Assessing properties of alkali activated GGBS based self-compacting geopolymer concrete using nano-silica. Case Studies in Construction Materials, 12, e00352. https://doi.org/10.1016/j.cscm.2020.e00352

Sargaphuti, M., Shah, S. P., & Vinson, K. D. (1993). Shrinkage cracking and durability characteristics of cellulose fiber reinforced concrete. ACI Materials Journal, 90(4), 309–318.

Selvarani, B., & Preethi, V. (2021). Investigational study on optimum content of GGBS and fibres in fibre non-breakable self compacting concrete. Materials Today: Proceedings, 47, 6111–6115.

Sireesha, N., & Madhavi, B. (2018). An experimental study on strength properties of GGBS and metakaolin in addition with alkaline solution of sodium hydroxide and sodium silicate. Anveshana's International Journal of Research in Engineering and Applied Sciences, 3, 96–102.

Stutzman, P. (2003). Development of an ASTM standard test method on X-ray powder diffraction analysis of hydraulic cements. In Proceedings of the 52nd Annual Denver X-ray Conference (pp. 4–7).

Verma, M., & Dev, N. (2022). Effect of ground granulated blast furnace slag and fly ash ratio and the curing conditions on the mechanical properties of geopolymer concrete. Structural Concrete, 23(4), 2015–2029. https://doi.org/10.1002/suco.202000536

Vinothkumar, A., Kalaivani, M., & Easwaran, P. (2019). Development of fly ash GGBS based self compacting geopolymer concrete: A review. International Research Journal of Multidisciplinary Technovation, 1(6), 373–377.

Vishnu, N., Kolli, R., & Ravella, D. P. (2021). Studies on self-compacting geopolymer concrete containing flyash, GGBS, wollastonite and graphene oxide. Materials Today: Proceedings, 43, 2422–2427.

COPYRIGHTS

©2023 The author(s). This is an open access article distributed under the terms of the Creative Commons Attribution (CC BY 4.0), which permits unrestricted use, distribution, and reproduction in any medium, as long as the original authors and source are cited. No permission is required from the authors or the publishers.

HOW TO CITE THIS ARTICLE

Keshavarzi, M., Pourrostam, T. & Javaheri Tafti, M. R. (2026). An Intelligent Approach Using the Experimental Study of Geopolymer Self-Compacted Concrete and Implementing an Intelligent Image Processing Techniques for the Rehabilitation of Building. (e743890). International Journal of Urban Management and Energy Sustainability, 7(2), e743890

DOI: 10.22034/ijumes.2026.743890